ORIGINAL ARTICLE

Synthesis and characterization of ZnO nanoparticles using aqueous extract of *Becium grandiflorum* for antimicrobial activity and adsorption of methylene blue

Mebrahtu Hagos Kahsay[1] ●

© The Author(s) 2021

Abstract

Nanotechnology is a recent field of modern research dealing with synthesis, strategy and manipulation of particle's structure in size range of 1–100 nm. This study introduces one of the methods of synthesis of nanoparticles, i.e., green synthesis of ZnO NPs using aqueous leaf extract of *Becium grandiflorum* (AM: 'Yedegamentisie'). The biomolecules of the plant extract (such as phenols, flavonoids, saponins, glycosides, steroids, tannins and alkaloids) were used as capping and reducing agent during synthesis of ZnO NPs. Response surface methodology coupled with Box-Behnken design (RSM-BBD) was used to optimize the synthesis of ZnO NPs and adsorption studies of the as-synthesized ZnO NPs. Then, ZnO NPs was characterized using different spectroscopic and microscopic instruments such as UV–Vis spectroscopy, FTIR, XRD and SEM–EDS to consider its purity, shape and crystallinity. UV–Vis analysis showed peaks in the range 305–312 nm due to synthesis of ZnO NPs. FTIR analysis showed the availability of different phytochemicals in the plant extract and synthesis of ZnO NPs at 490 cm^{-1}. Powder XRD patterns confirmed formation of phase pure wurtzite structures of ZnO NPs. The synthesized ZnO NPs were used to remove MB dye from aqueous solution by acting as a photocatalyst and adsorbent as well as, it also showed antimicrobial activity against two gram positive (*Staphylococcus epidermidis*, *Staphylococcus aureus*) and three gram negative (*Escherichia coli*, *Klebsiella pneumonia*, *Pseudomonas aeruginosa*) bacteria.

Introduction

Cosmetic, food, leather, paper, plastics and textile industries use extensively different types of dyes and pigments to color their products. Textile industries in particular generate 100–170 L dye effluent per Kg of cloth (Mohan et al. 2007). Effluents contaminated with dyes that are discharged into oceans, seas, rivers and ponds from textile factories and the like can bring disturbance to the water eco-system due to two main reasons, i.e., toxic properties of the dyes and blockage of sun light to reach the plankton in the water system.

Dyes are aromatic compounds that have delocalized electron systems that can bind with a material to give color in textile factories (Velmurugan et al. 2011). Methylene blue

(MB) was first synthesized in 1876 for use in the textile industry (Berneth 2005). MB is a cationic dye and is commonly used for coloring paper, temporary hair colorant, dyeing cotton wools and so on (Pirkanniemi and Sillanpää 2002). MB is a dye that was synthesized and tested as anti-malarial drug before the twentieth century (Schirmer et al. 2003). MB is also used in combination with amodiaquine for falciparum malaria in African adults and children (Mandi et al. 2005; Meissner et al. 2006; Zoungrana et al. 2008).

Effluents from textile, paper and pharmaceutical industries containing MB pollute water bodies that adversely affect the eco-system and aquatic life. Inhaling or presence of MB in drinking water is a health hazard as it causes eye and skin irritation, hemolytic anemia, diarrhea and nausea, difficulties in breathing, vomiting and abdominal pain are among the symptoms that can occur in humans (Pirkanniemi and Sillanpää 2002). Now a days about 700 million people of our globe have faced water scarcity for both drinking and domestic purposes due to water pollution mostly from anthropogenic activities, and it is still estimated that people faced these problem will

✉ Mebrahtu Hagos Kahsay
mebrahtuh@wldu.edu.et; hagosmebrahtu@gmail.com

1 Department of Chemistry, Woldia University, P.O.BOX 400, Woldia, Ethiopia

Table 1 The experimental levels of factors used for RSM-BBD optimization

Name	Type	Changes	SD	Low	High
Zinc acetate (mM)	Factor	Easy	0	1	5
Plant extracts conc. (%)	Factor	Easy	0	1	5
pH	Factor	Easy	0	3	11
Absorption maximum (nm)	Response		3.93247	298	313

increase to 1.8 billion people by 2025 (Water for life: International Decade of Action Begins 2005). According to a World Health Organization (WHO) report, water borne diseases lead to death of nearly 12 million people mostly in developing countries each year (World Health Organization. Regional Office for Europe & International Federation of Red Cross and Red Crescent Societies 2001). Dyes such as MB or cationic pharmaceuticals have been treated from industrial effluents/waste water using adsorbents such as poly (vinyl alcohol) (PVA) (Roufegari-Nejhad et al. 2019), activated carbon (Gimba et al. 2001) and activated charcoal (Zhao et al. 2018) had been reported. Similarly, TiO$_2$/UV-C photocatalytic process using batch reactor in removing MB from textile synthetic wastewater had been studied by (Rahimi et al. 2013). Omar et al. (2014) reported the use of zinc oxide/reduced graphene oxide (ZnO/rGO) nanocomposites (NCs) as both adsorbent and photocatalyst for removal of MB from aqueous solution, while Kahsay et al. (2020) used magnetic rGO/Fe$_3$O$_4$ NCs as adsorbent to remove crystal violet dye from aqueous solution.

Synthesis of nanoparticles using biological means has become a new trend in nanoparticle production due to the following advantages: non toxicity, large scale production without the presence of impurities, easy scaling-up, well-defined morphology and has been used as drug carriers, cosmetics and fillings in medical materials (Rosi and Mirkin 2005; Singh et al. 2016; Yuvakkumar et al. 2014). The photochemicals such as proteins, amino acids, organic acid, vitamins, as well as secondary metabolites, such as flavonoids, alkaloids, polyphenols, terpenoids, heterocyclic compounds and polysaccharides, have significant roles in metal salt reduction, and furthermore, act as capping and stabilizing agent for synthesis of nanoparticles (Duan et al. 2015). There are few already identified chemical constituents of plant extracts such as catechin, gallic acid and coumaric acid that have been played a great role in reducing zinc acetate to ZnO NPs (Salam et al. 2014). Some authors have mentioned the role of capping ligand is crucial in preventing agglomeration when ZnO NPs are synthesized by precipitation and sol–gel methods. The-OH functional groups of starch and polyethylene glycol (PEG) molecules bind with the surface of ZnO NPs and cap it (Balcha et al. 2016).

Hence, the researcher has used leaf extract of *Becium grandiflorum* to synthesize ZnO NPs and the as-synthesized

ZnO NPs was used for multi applications as adsorbent and photocatalyst to remove MB dye from aqueous solution and as bactericidal against both gram positive and gram negative bacteria.

Experimental

Chemicals

All chemicals used are analytical grade. Zn(CH$_3$COO)$_2$•2H$_2$O was bought from Chemicals UDYOG-12001 (India), NaOH was acquired from (JHD, China), MB (C$_{16}$H$_{18}$ClN$_3$·xH$_2$O) was bought from (Abron chemicals, India), HCl (37%) was acquired from (Pentokey, India), CHCl$_3$ was bought from (Blulux, India), leaves of *Becium grandiflorum* were collected from Yemrehane Kristos church forest (North Wollo, Ethiopia), and deionized water was used to prepare solutions through out of the experiments.

Preparation of aqueous leaf extract of *Becium grandiflorum*

The leaves of *Becium grandiflorum* were collected and rinsed with distilled water to remove dust and impurities from the surface of the plant. Then, the leaves were allowed to shed dry at room temperature for 14 days. After drying, the leaves were crushed in to powder with grinder and allowed to pass through 1.4 mm mesh. Finally to prepare 1% plant extract, 1 g leaf powder was immersed in to 100 mL deionized water and heated at 40 °C for 20 min. After cooling, the solution was filtered with Whatman no. 1 filter paper, and extract was collected in volumetric flask for further use.

Qualitative phytochemical analysis of leaf extract of *Becium grandiflorum*

The phytochemical screening of *Becium grandiflorum* was studied based on the procedure in our previous study (Gebremedhn et al. 2019).

Synthesis of ZnO nanoparticles

ZnO NPs were synthesized using biological approach using Zn(CH$_3$COO)$_2$•2H$_2$O precursor and aqueous leaf extract of *Becium grandiflorum* as reducing and capping agent. The synthesis procedure was optimized (RSM-BBD) using different variables, i.e., Zn(CH$_3$COO)$_2$•2H$_2$O, percent of leaf extract, temperature and reaction time. Best product was collected at the optimized condition of Zn(CH$_3$COO)$_2$•2H$_2$O, pH, leaf extract and reaction time corresponding to 1 mM, 9, 1%, 60 °C and 30 min, respectively. The synthesized product had pale yellow color indicating the formation of ZnO NPs.

Fig. 1 *Becium grandiflorum* **a** habitat and **b** qualitative phytochemical screening

The optimization procedure for the synthesis of ZnO NPs was designed by Design expert 11software and the experimental levels of factors used for RSM-BBD are given in Table 1 below.

Characterization of ZnO nanoparticles

To study the optical properties of the synthesized ZnO NPs, Ultraviolet–visible spectroscopy (UV–vis) (UV-2450, Shimadzu) was used in the wavelength range 200–800 nm. To identify the functional groups present in the plant extract and ZnO NPs, Fourier transform infrared (FTIR) spectrophotometer (Perkin-Elmer 1725x) in the range 4000–400 cm^{-1} was recorded by KBr pellet method. The crystallite size and XRD patterns of the as-synthesized ZnO NPs were determined using X-ray diffractometer (Perkin-Elmer spectrum one instrument) Cu–Kα radiations ($\lambda = 0.15406$ nm) in 2θ range from 20º to 100º, and morphology of the as-synthesized ZnO NPs was characterized using Scanning electron microscopy (SEM, Zeiss ultra-60) equipped with x-ray energy dispersive spectroscopy (EDS).

RSM-BBD as a method of optimization of synthesis of ZnO NPs and adsorption process

Optimization parameters were designed by Design Expert 11 software for both synthesis and later adsorption of MB dye using ZnO NPs in order to minimize the cost, time and energy. During synthesis, there are three factors/variables (Zinc acetate, plant extract concentration and pH), while the response is absorption maximum of ZnO NPs. First plant extract (1–5%) is immersed to zinc acetate solution (1–5 mM) in a conical flask and the pH of the mixed solution is adjusted to pH (3, 7, 11) using 0.1 M HCl/0.1 M NaOH solution. Then, the reaction was allowed to react for 30 min at 60 °C, while agitating the reaction mixture at 1000 rpm. However, the adsorption parameters are three variables, i.e., ZnO NPs dose (mg), contact time (min) and initial MB concentration (mg/L), whereas the response is dye removal (%). Selected ZnO NPs dose variables were (25, 62.5, 100 mg); contact time (0–180 min) and initial MB concentration were (25, 65.5, 100 mg/L).

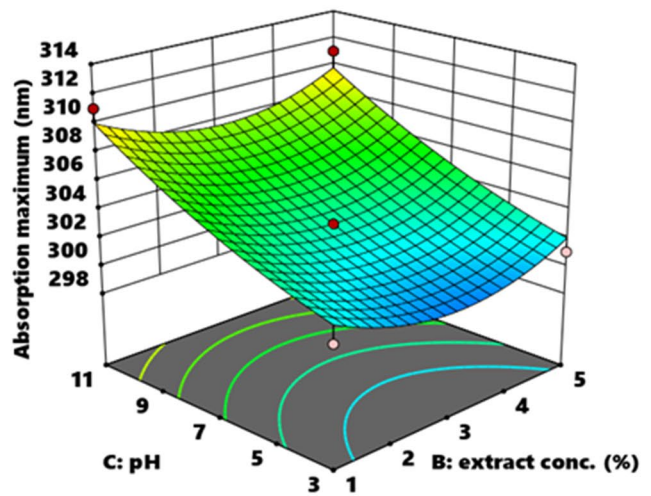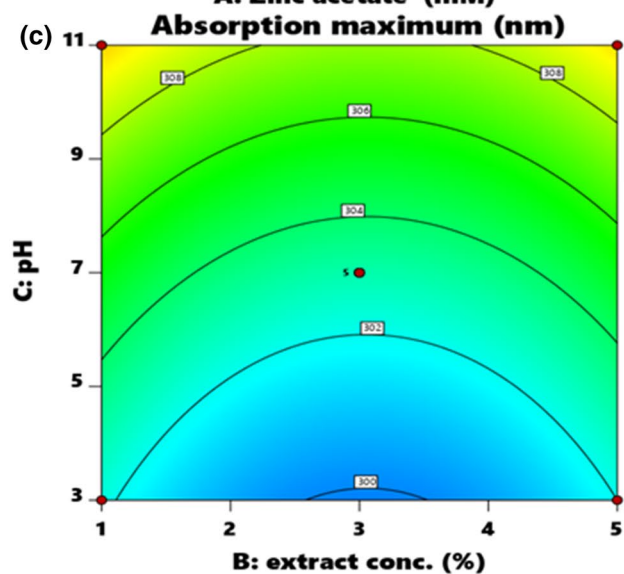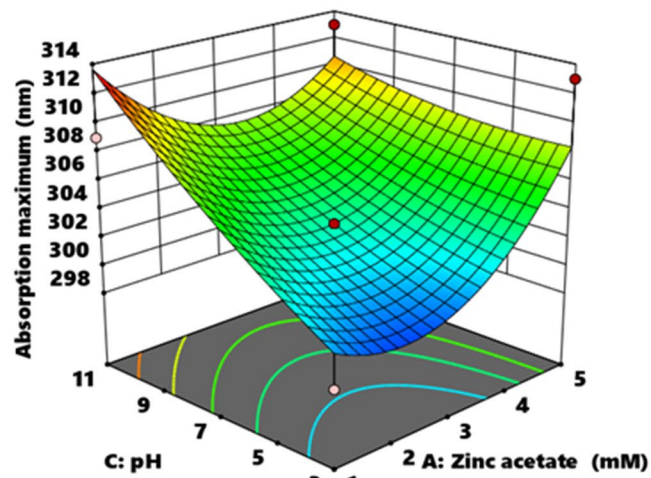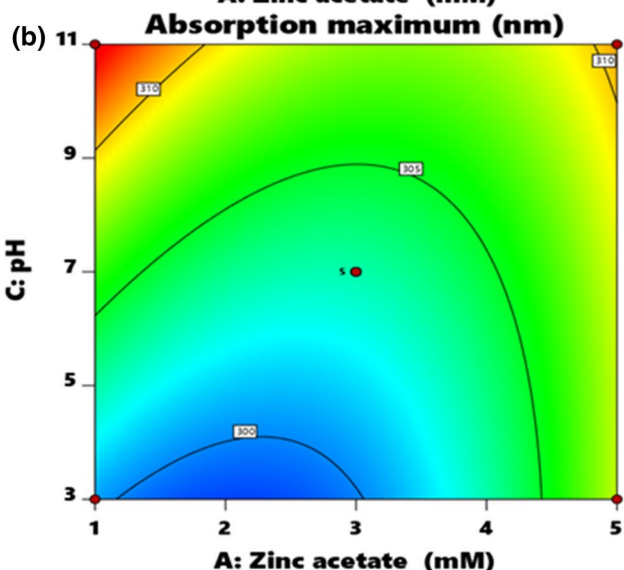**Fig. 2** Synthesis of ZnO NPs at different concentrations of precursor and pH
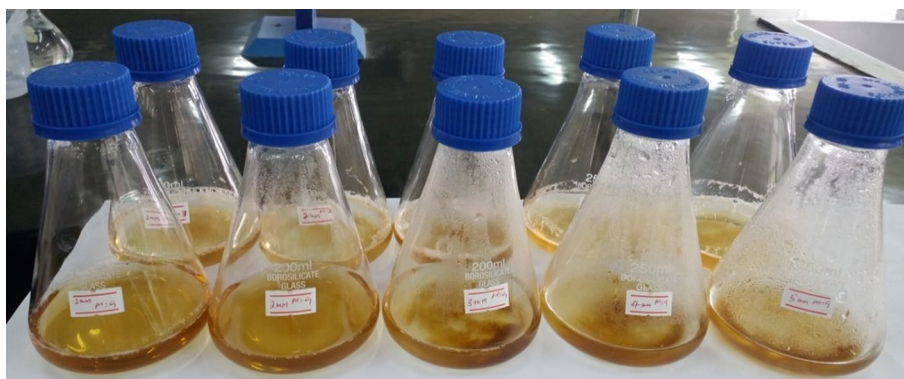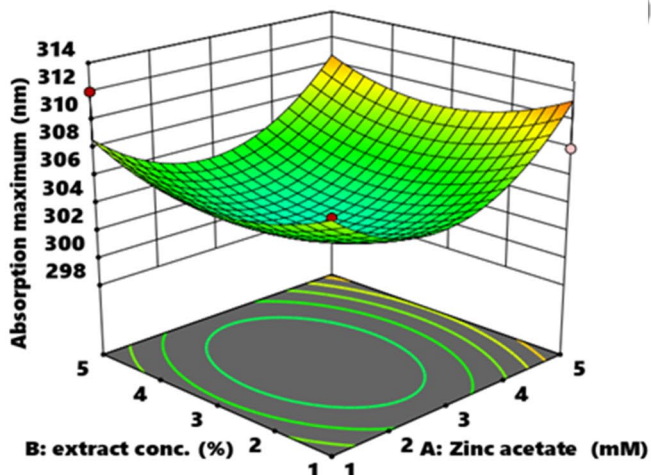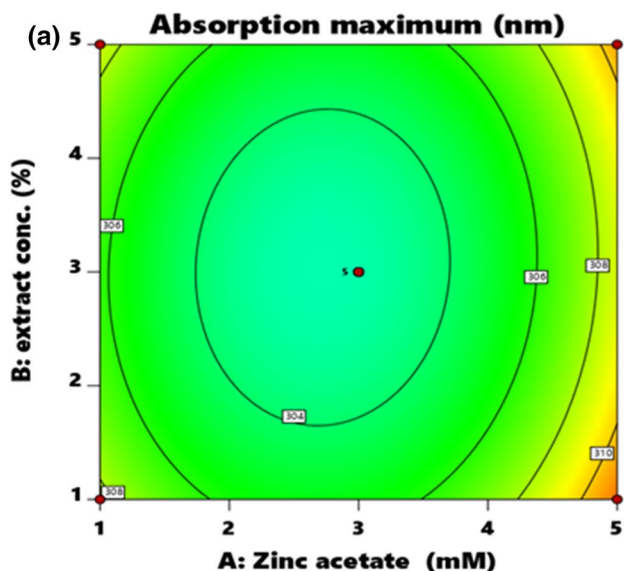
◀**Fig. 3** The 2D-3D surface plots of the effect of factors **a** plant extract conc. % and zinc acetate conc., **b** pH and zinc acetate conc., and **c** pH and plant extract conc. %

Photocatalytic activity of ZnO NPs

The photocatalytic efficiency of the as-synthesized ZnO NPs was conducted in a batch reactor under UV photo irradiation and MB as a model organic dye pollutant at various conditions of initial dye concentration, ZnO NPs dose and pH. At the adsorption–desorption equilibrium, 3 mL of the colloidal suspension was taken into a clean vial and labeled as 0 min. Similarly, subsequent batches at every 20 min were irradiated with UV light, and then, the absorption of each solution was measured in the wavelength range 200–800 nm using UV–vis spectroscopy and the percentage of dye degradation (%) was calculated using Eq. (1).

$$\text{Dye degradation}(\%) = (C_o - C)/C_o \times 100 \tag{1}$$

where 'C_o' and 'C' are initial and equilibrium concentration of MB dye (ppm), respectively.

Antibacterial activity screening

The antimicrobial activity of ZnO NPs was evaluated against two gram positive (*Staphylococcus epidermidis*, *Staphylococcus aureus*) and three gram negative (*Klebsiella pneumonia*, *Pseudomonas aeruginosa*, *Escherichia coli*) bacteria by agar well diffusion method (Bonev et al. 2008). Mueller Hinton agar medium was adjusted to pH 7 with 1 N NaOH and distilled water to form 1 L solution. The standardized culture of test bacteria was first evenly spread onto the surface of Mueller Hinton agar plates using sterile cotton swabs. Four wells (6 mm) were made in each plate with sterile cork borer. Wells were filled with 50 µL of ZnO NPs at the concentrations of (2.5, 5, and 10 mg/mL). In the remaining well, 50 µL of Gentamicin (as positive control) was added to each plate. All the plates were then covered with lids and incubated at 37 °C for 24 h. The size of inhibition zones was measured, and antimicrobial activity of the ZnO NPs was expressed in terms of the average diameter of inhibition zone in mm.

Results and discussion

Phytochemical screening of *Becium grandiflorum*

Prior to synthesis of ZnO NPs the qualitative photochemical screening of the plant (Fig. 1a) was studied using different chemicals and procedures. Based on the results the phytochemicals found in aqueous leaf extract of *Becium*

grandiflorum were phenols, flavonoids, saponins, glycosides, steroids, tannins and alkaloids (Fig. 1b). These bioactive molecules are believed to reduce $Zn(CH_3COO)_2 \bullet 2H_2O$ and cap the as-synthesized ZnO NPs afterward to control growth and avoid agglomeration of the nanoparticles.

Characterization of ZnO NPs

Aqueous leaf extract of *Becium grandiflorum* showed characteristic peak at 315 nm due to $n \rightarrow \pi^*$ or $\pi \rightarrow \pi^*$ transitions of carbonyls, C=C or molecules with heteroatoms functional groups from the plant extract. The prepared plant extract was used to synthesize ZnO NPs which was acted as both reducing and capping agent. The UV–vis spectrum results showed the production and distribution of ZnO NPs using different concentrations of $Zn(CH_3COO)_2 \cdot 2H_2O$ precursor (1, 2, 3, 4, 5 mM), pH and time of reaction that showed maximum absorption at 312, 311, 303, 305 and 308 nm, respectively due to synthesis of ZnO NPs at pH = 9 (Fig. 2) and (Fig. 3). Therefore, ZnO NPs using leaf extract of *Becium grandiflorum* showed minimum absorption peak at 303 nm that had resulted calculated particle size of 1.35 nm using effective mass model and oversimplified mathematical equation, Eq. (2) derived by (Brus 1986). Similarly, (Talam et al. 2012) reported synthesis of ZnO NPs via precipitation method that has a size of 2.07 nm according to the equation below. Hence, size of the synthesized nanoparticles decreased with decrease in the wavelength absorption maximum of nanoparticles (particle size and plasmon resonance absorbance are directly proportional to each other).

The surface plots of the response using the three factors, i.e., concentration of zinc acetate, % of plant extract and pH to obtain optimized absorption maximum of the synthesized ZnO NPs using 2D-3D plots is represented in Fig. 3.

$$r(\text{nm}) = \frac{-0.3049 + \sqrt{-26.23012 + 10240.72/\lambda_p(\text{nm})}}{-6.3829 + 2483.2/\lambda_p(\text{nm})} \tag{2}$$

where 'r' is the particle radius and 'λ_p' is peak absorbance wavelength in nm.

Increasing the concentration of the precursor from 1 to 5 mM increased the absorption intensity and wavelength from 298 to 303 nm in acidic medium (pH = 3). Whereas in basic medium (pH = 9) increasing precursor concentration decreased the intensity and wavelength from 312 to 308 nm as in Fig. 3. Synthesis of ZnO NPs was more favored in basic condition (pH = 9) by using minimum concentration of the precursor. More numbers of ZnO NPs were produced at lower concentration of the precursor in basic medium due to precipitation reaction.
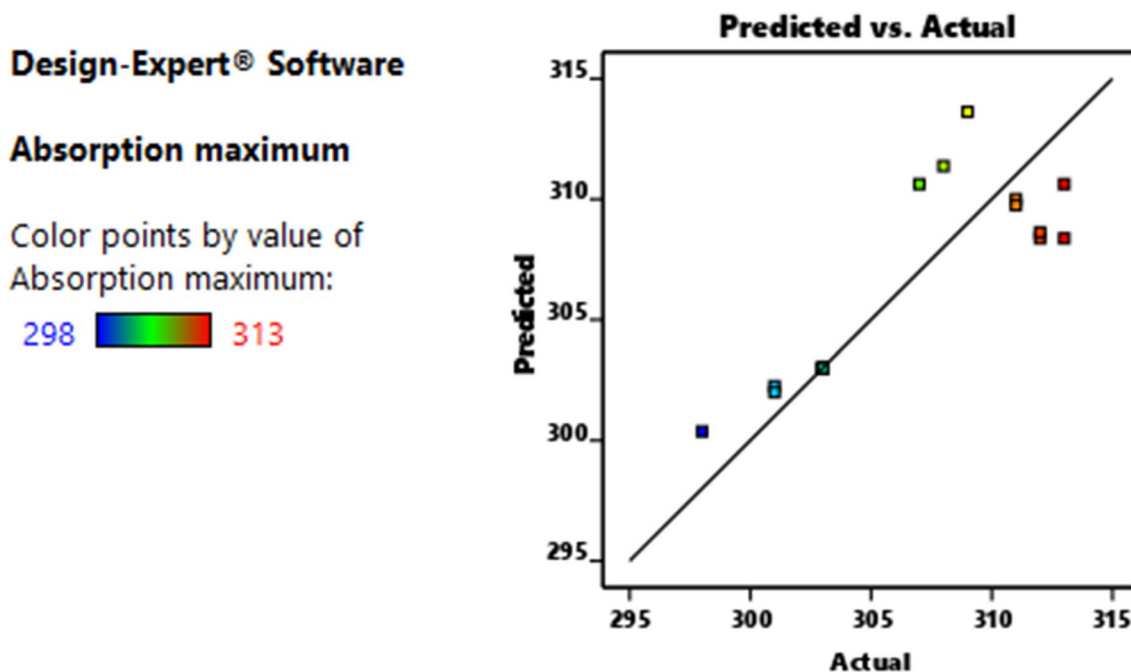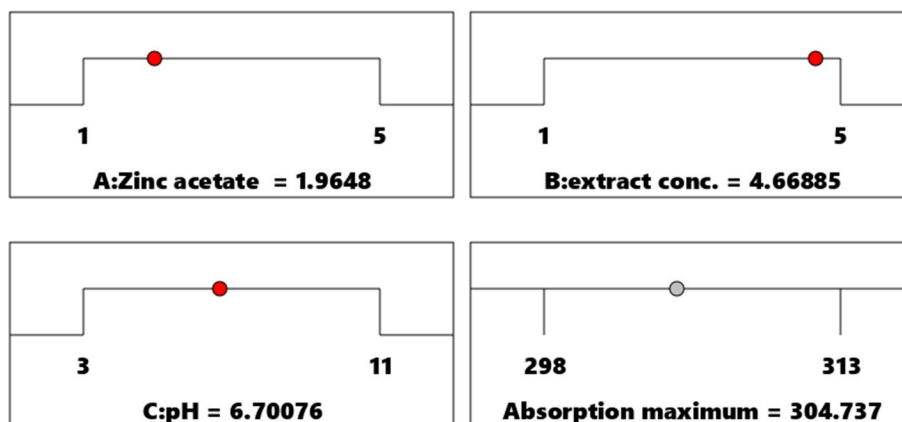
Predicted vs. Actual

Design-Expert® Software

Absorption maximum

Color points by value of
Absorption maximum:

298 ████████ 313

Fig. 4 Comparison of ZnO NPs wavelength absorption maximum between predicted and actual

Fig. 5 The desirability ramp for the optimization of three factors (viz. Zinc acetate conc., plant extract conc. and pH) to yield best absorption maximum for ZnO NPs

A:Zinc acetate = 1.9648

B:extract conc. = 4.66885

C:pH = 6.70076

Absorption maximum = 304.737

Desirability = 1.000
Solution 1 out of 100

Figure 4 shows correlation between predicted (model) $R^2 = -3.4612$ and adjusted (actual) $R^2 = 0.3627$. A negative predicted R^2 implies that the overall mean may be a better predictor of your response than the current model. The desirability ramp to yield best absorption maximum for ZnO NPs is shown in Fig. 5.

Figure 6 shows FTIR spectra of both leaf powder of *Becium grandiflorum* and ZnO NPs. Leaf powder of *Becium*

grandiflorum shows characteristic peaks at 3334, 2915, 1635, 1410, 1261, 1043 and 609 cm^{-1} due to OH stretching, sp^3 C–H stretching, C=C stretching, C–H bending, C–N or phenols, C–O stretching and C-H bending (C=C–H), respectively, whereas ZnO NPs using leaf extract of *Becium grandiflorum* shows characteristic peaks at 3378, 2915, 1560, 1500, 1380, 1043, 939, 826, 691 and 490 cm^{-1} due to OH stretching, C–H stretching of alkane, C=C aromatic ring,
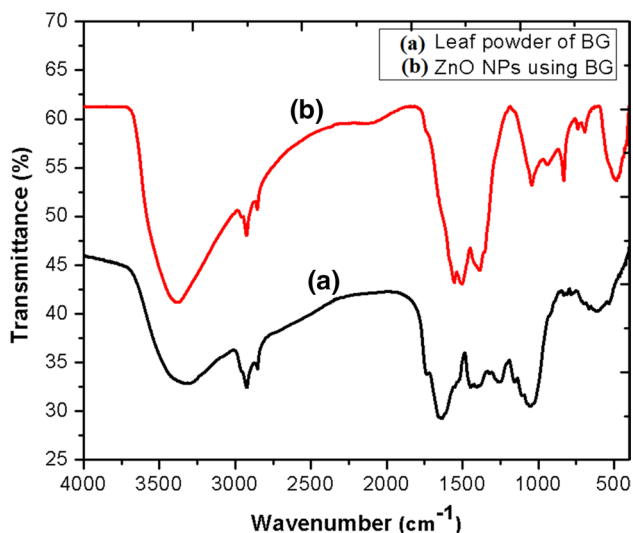
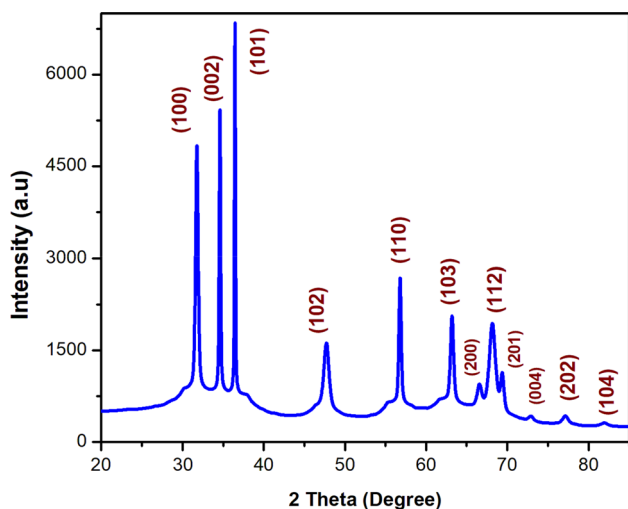Fig. 6 FTIR of leaf powder of *Becium grandiflorum* and ZnO NPs

Fig. 7 Powder XRD of ZnO NPs using leaf extract of *Becium grandiflorum*

O–N = O nitro group, C–O stretching, C–N stretching, meta disubstitute ring and Zn–O stretching due to formation of ZnO NPs, respectively.

The phase purity and crystallinity of the as-synthesized ZnO NPs were studied using powder x-ray diffractometer, Fig. 7. The XRD patterns of ZnO NPs show 2θ values at 31.74°, 34.58°, 36.43°, 47.71°, 56.79°, 63.20°, 66.58°, 68.18°, 69.40°, 72.96°, 77.13° and 81.92° corresponding to (100), (002), (101), (102), (110), (103), (200), (112), (201), (004), (202) and (104) planes of hexagonal wurtzite structure (JCPDS card no.: 36-1451) (Tao et al. 2008)). The average crystallite size (D) of ZnO NPs using the Debye–Sherrer formula, Eq. (3) using the intense peak at (101) was calculated to be 20 nm.

$$D = \frac{0.9\lambda}{\beta cos\theta} \tag{3}$$

where 'D' is the crystallite size (nm), 'λ' is the wavelength of Cu kα radiation ($\lambda = 0.15406$ Å), and 'β' is the full width at half maximum of the diffraction peak (in radians).

The morphology of the as-synthesized ZnO NPs was studied using SEM. Figure 8a, b shows SEM image of the as-synthesized ZnO NPs and EDS image of ZnO NPs. EDS image confirmed the elemental composition of ZnO NPs. The percent composition of Zn and O in ZnO NPs was 40.38 and 59.62% by atomic mass, respectively, confirmed synthesis of ZnO NPs.

Adsorption property of ZnO NPs

RSM-BBD was applied to obtain maximum dye removal efficiency using the as-synthesized ZnO NPs as an adsorbent (Fig. 9). The three independent variables involved according to BBD matrix are ZnO NPs dose (A), contact time (B) and initial MB concentration (C), whereas the response is adsorption (Y), Eq. (4). The quadratic model equation for adsorption capability of ZnO NPs in this study is represented as
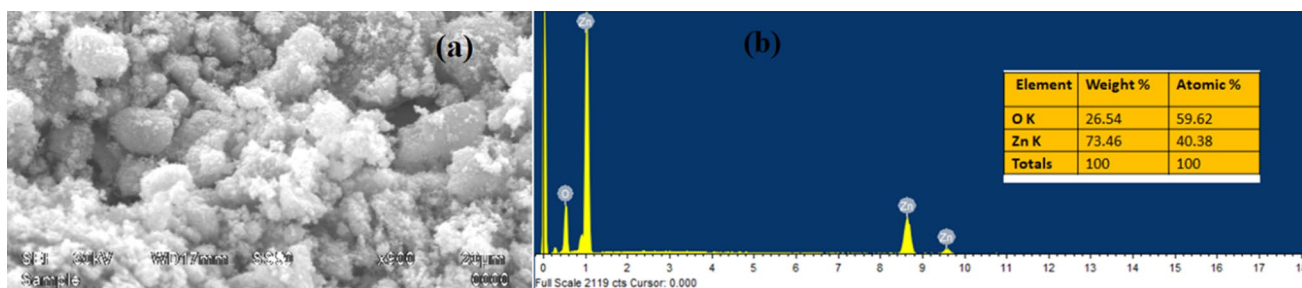

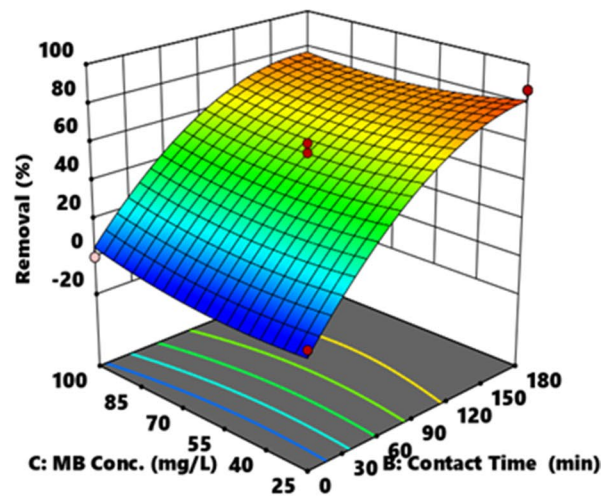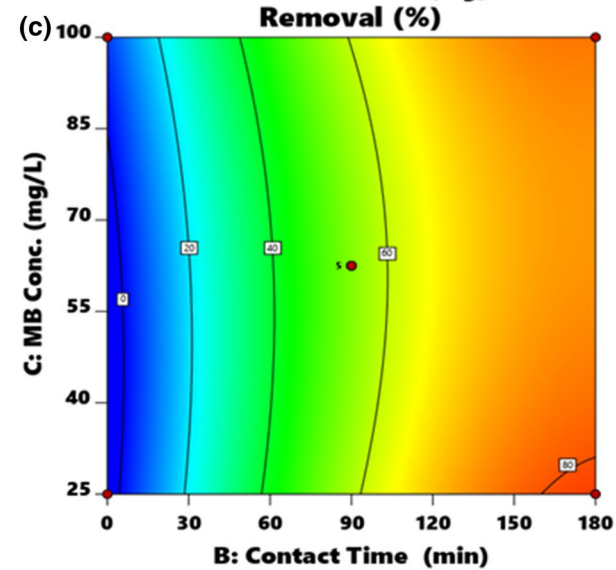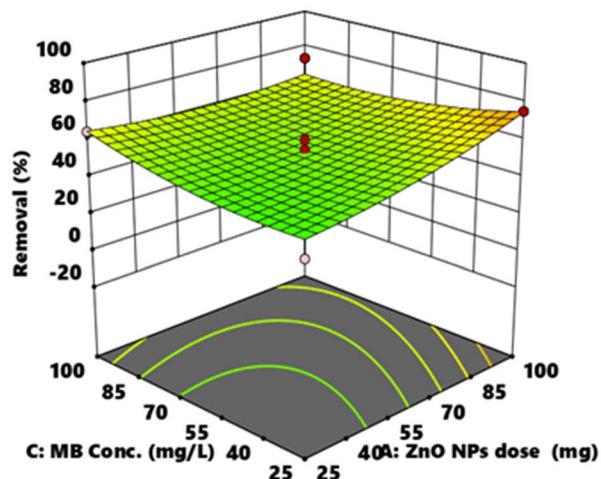Fig. 8 a SEM image and b EDS spectrum of ZnO NPs

Element	Weight %	Atomic %
O K	26.54	59.62
Zn K	73.46	40.38
Totals	100	100

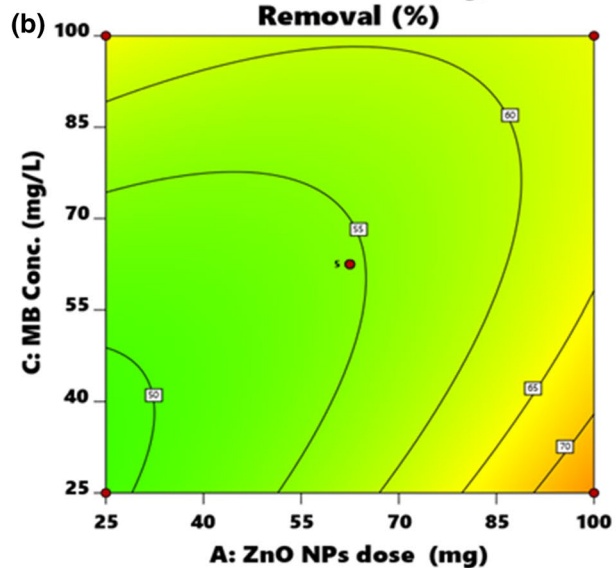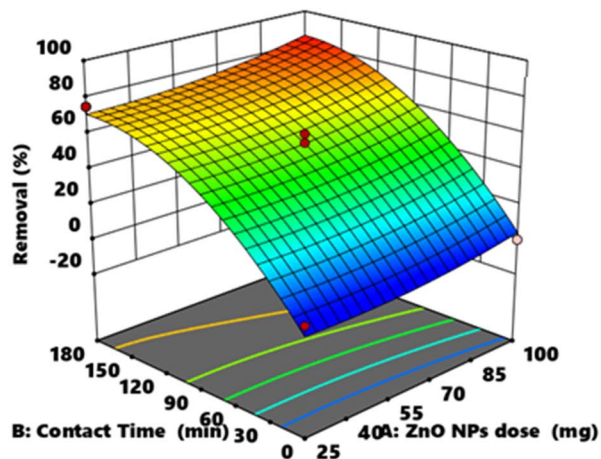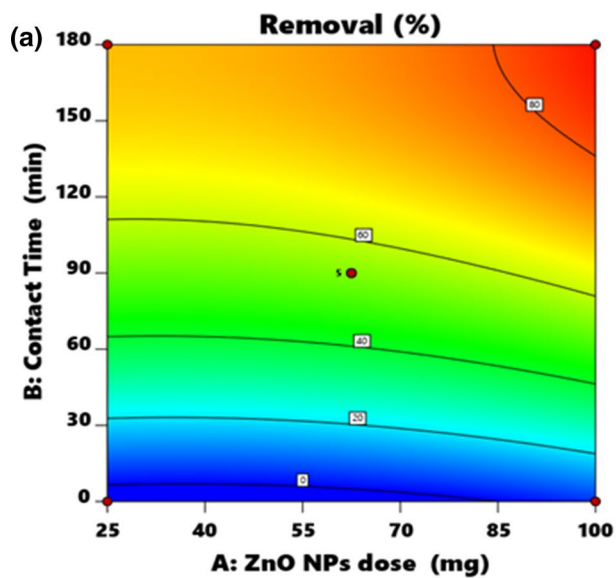**(a)**

(b)

(c)

◂**Fig. 9** The 2D-3D surface plots of the effects of **a** ZnO dose NPs vs contact time, **b** ZnO NPs dose vs MB conc and **c** contact time vs MB conc for dye removal efficiency (%) using the as-synthesized ZnO NPs

$$
\begin{aligned}
\text{Adsorption}(Y) =\ & 54.60 + 6.09A + 39.38B + 1.04C \\
& + 1.25AB - 6.58AC - 3.50BC \\
& + 3.61A^2 - 19.46B^2 + 4.86C^2
\end{aligned}
\tag{4}
$$

In the above equation, positive coefficients increase ZnO NPs adsorption, while negative coefficients affect inversely ZnO NPs adsorption. The Table 2 below shows coefficients in terms of coded factors. Percent of dye removal was calculated to be 71.53% when the adsorbent mass and dye concentration are 25 mg and 25 mg/L, respectively (Fig. 10). *Becium grandiflorum* mediated ZnO NPs showed adsorption maximum of 143.6 mg MB/g ZnO NPs adsorbent in this study. Other reports demonstrated ZnO NPs have a removal capacity of 10.70 ± 0.80 mmol/g of MB from aqueous solution (Zhang et al. 2013). Similarly, sawdust-derived cellulose nanocrystals (CNC) incorporated with ZnO nanocomposite showed maximum adsorption capacity of 64.93 mg/g toward MB (Oyewo et al. 2020).

Photocatalytic degradation of ZnO NPs

The as-synthesized ZnONPs was used as a catalyst to degrade a model organic dye pollutant, i.e., MB under UV photo irradiation.

The maximum absorption of the dye was observed at 664 nm. 100 ml (100 ppm) MB dye was photodegraded using 0.5 g L^{-1} of ZnO NPs photocatalyst. MB dye was 69% degraded after 200 min (Fig. 11a) and reaction rate constant (k) for degradation of MB were calculated to be 1.9×10^{-3} min^{-1} and $R^2 = 0.983$ (Fig. 11b). However, the reaction rate constant for the photocatalytic degradation of MB using ZnO nanostructures was reported to be 9.14×10^{-3} min^{-1} (Kahsay et al. 2019). Similarly, in another work MB dye is photocatalytically degraded to 99% at room temperature using 50 mg dose of RGO-Ag/ZnO nanocomposite in the presence of H_2O_2 (Belachew et al. 2020). The kinetic study of the catalytic degradation of MB dye using the ZnO NPs was performed using the Langmuir–Hinshelwood–Hougen–Watson (LH–HW) kinetic model, Eq. (5).

$$
-r_A = \frac{kC_A}{(1 + kC_A)}
\tag{5}
$$

where 'r_A' is the rate of consumption of MB dye (mol dm^{-3} s^{-1}), 'C_A' is an MB dye concentration (mol dm^{-3}), and 'k' is the rate constant.

The photogenerated charge carriers (h^+ in the valence band and e in conduction band) are able to interact with the adsorbed MB dye to form hydroxyl or superoxide radicals to facilitate the degradation of MB dye molecules to CO_2 and water (Herrmann et al. 1997); (Vignesh et al. 2012).

Antimicrobial activity

Figure 12 shows the antibacterial activity of ZnO NPs against gram positive and gram negative bacteria using standard well-diffusion. The higher zone of inhibition was measured to be 12 mm by *Staphylococcus epidermidis*, whereas *Staphylococcus aureus, Escherichia coli, Klebsiella pneumonia* and *Pseudomonas aeruginosa* showed minimum zone of inhibition of 7, 6, 8 and 11 mm, respectively. The release of Zn^{2+} from ZnO NPs is one of the main propositions in antibacterial mechanisms which are known to inhibit several bacterial cells activities (such as active transport, bacteria metabolism and enzymes activity) which leads to the formation of reactive oxygen species (ROS) which leads to oxidative stress and subsequent cell damage or death (Soren et al. 2018).

Conclusions

ZnO NPs was successfully synthesized by using leaf extract of *Becium grandiflorum*. Based on the FTIR results phytoconstituents such as phenols, flavonoids, saponins, glycosides, steroids, starch, tannins and alkaloids were used as both reducing and capping agent. Similarly, synthesis of ZnO NPs was confirmed by showing characteristic peak at 490 cm^{-1}. The as-synthesized ZnO NPs showed adsorbent and phtotocatalytic property to remove MB dye from aqueous solution. Adsorption behavior best fitted to Langmuir isotherm with $r^2 = 1$ and $q_{max} = 143.6$ mg MB/g ZnO NPs adsorbent (*not shown here*). Maximum percent of MB dye removal was calculated 71.53% when the adsorbent mass and dye concentration were 25 mg and 25 mg/L, respectively, at 180 min. Similarly, ZnO NPs degraded MB by 69% within 200 min. Moreover, ZnO NPs showed antimicrobial property against five standard bacteria strain and showed maximum zone of inhibition of 12 mm by *Staphylococcus epidermidis*. Hence, ZnO NPs using leaf extract of *Becium grandiflorum* has a potential to remove organic

Table 2 Coefficients in terms of coded factors

Factor	Coefficient estimate	df	Standard error	95% CI low	95% CI High	VIF
Intercept	54.60	1	3.41	46.54	62.66	
A-ZnO NPs dose	6.09	1	2.69	− 0.2814	12.46	1.0000
B-contact time	39.38	1	2.69	33.01	45.74	1.0000
C-MB conc.	1.04	1	2.69	− 5.33	7.41	1.0000
AB	1.25	1	3.81	− 7.76	10.26	1.0000
AC	−6.58	1	3.81	− 15.58	2.43	1.0000
BC	−3.50	1	3.81	− 12.51	5.51	1.0000
A^2	3.61	1	3.71	− 5.17	12.39	1.01
B^2	−19.46	1	3.71	− 28.24	− 10.68	1.01
C^2	4.86	1	3.71	− 3.92	13.64	1.01

Fig. 10 The desirability ramp for the optimization of three factors (viz. ZnO NPs dose, contact time and MB conc.) to yield maximum dye removal (%) using the as-synthesized ZnO NPs adsorbent
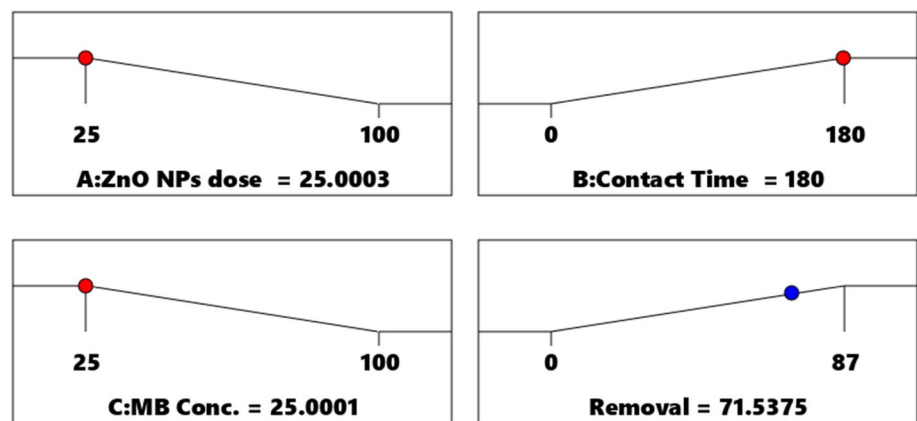
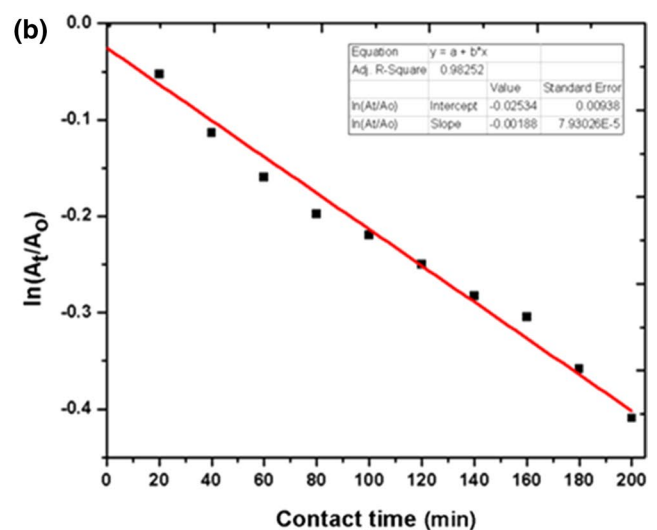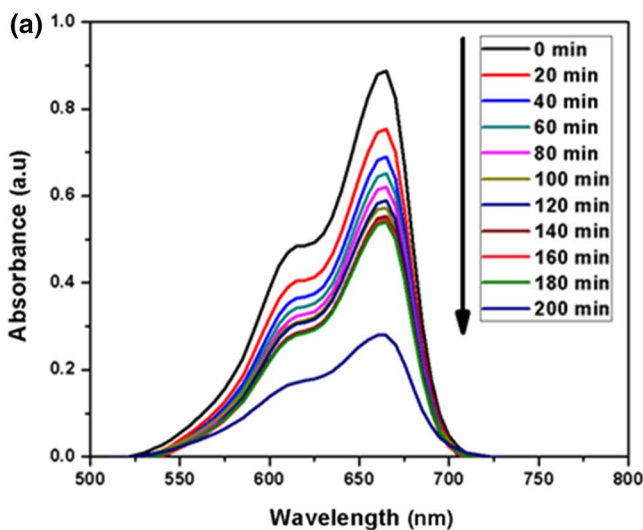

Desirability = 0.952
Solution 1 out of 32

Fig. 11 a Photocatalytic degradation of MB using ZnO NPs catalyst and **b** pseudo first order kinetics
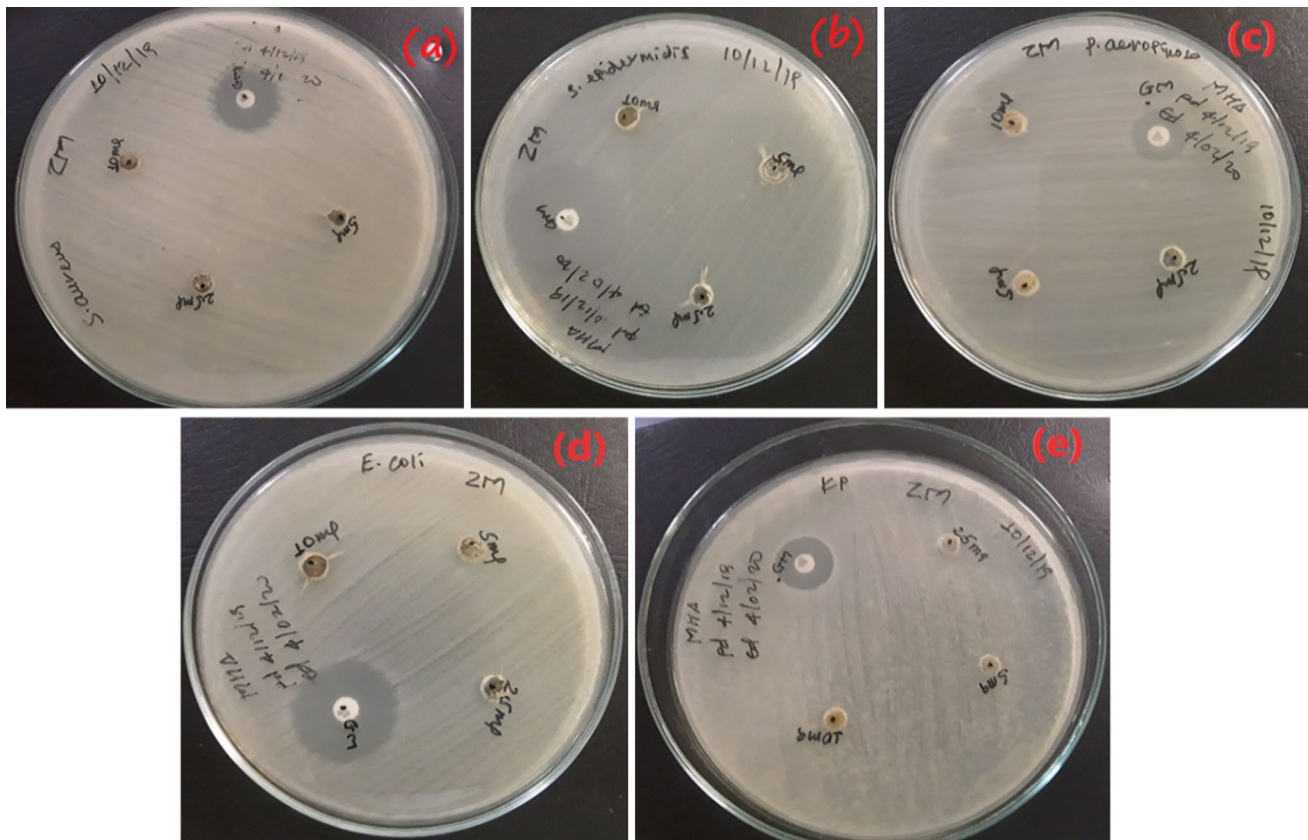
Fig. 12 Antimicrobial activities of ZnO NPs against **a** *Staphylococcus aureus*, **b** *Staphylococcus epidermidis*, **c** *Pseudomonas aeruginosa*, **d** *Escherichia coli* and **e** *Klebsiella pneumonia*

dye pollutants and pathogenic bacteria from contaminated water.

Compliance with ethical standards

Conflict of interest The author declares that he has no conflict of interest.

Data availability The author declares that the data supporting the findings of this study are available within the article, and other supplementary data are available from the corresponding author upon request.

References

Belachew N, Kahsay MH, Tadesse A, Basavaiah K (2020) Green synthesis of reduced graphene oxide grafted Ag/ZnO for photocatalytic abatement of methylene blue and antibacterial activities. J Environ Chem Eng 8(5):104106–104113

Balcha A, Yadav OP, Dey T (2016) Photocatalytic degradation of methylene blue dye by zinc oxide nanoparticles obtained from precipitation and sol–gel methods. Environ Sci Pollut Res Int 23(24):25485–25493

Berneth H (2005) Azine Dyes. In: Ullmann's encyclopedia of industrial chemistry, electronic release, Wiley-VCH, Weinheim

Bonev B, Hooper J, Parisot J (2008) Principles of assessing bacterial susceptibility to antibiotics using the agar diffusion method. J Antimicrob Chemother 61(6):1295–1301. https://doi.org/10.1093/jac/dkn090

Brus L (1986) Electronic wave functions in semiconductor clusters: experiment and theory. J Phys Chem 90(12):2555–2560. https://doi.org/10.1021/j100403a003

Duan H, Wang D, Li Y (2015) Green chemistry for nanoparticle synthesis. Chem Soc Rev 44(16):5778–5792

Gebremedhn K, Kahsay MH, Aklilu M (2019) Green synthesis of CuO nanoparticles using leaf extract of catha edulis and its antibacterial activity. J Pharm Pharmacol 7(6):327–342. https://doi.org/10.17265/2328-2150/2019.06.007

Gimba CE, Olayemi JY, Okunnu ST, Kagbu JA (2001) Adsorption of methylene blue by activated carbon from coconut shell. Glob J Pure Appl Sci 7(2):265–268. https://doi.org/10.4314/gjpas.v7i2.16242

Herrmann J, Tahiri H, Aitichou Y, Lassaletta G, Gonzalezelipe A, Fernandez A (1997) Characterization and photocatalytic activity in aqueous medium of TiO2 and Ag-TiO2 coatings on quartz. Appl Catal B 13(3–4):219–228

Kahsay MH, Belachew N, Tadesse A, Basavaiah K (2020) Magnetite nanoparticle decorated reduced graphene oxide for adsorptive removal of crystal violet and antifungal activities. RSC Adv 10(57):34916–34927

Kahsay MH, Tadesse A, RamaDevi D, Belachew N, Basavaiah K (2019) Green synthesis of zinc oxide nanostructures and investigation of their photocatalytic and bactericidal applications. RSC Adv 9(63):36967–36981. https://doi.org/10.1039/c9ra07630a

Mandi G, Witte S, Meissner P, Coulibaly B, Mansmann U, Rengelshausen J, Schiek W, Jahn A, Sanon M, Wüst K, Walter-Sack I, Mikus G, Burhenne J, Riedel K-D, Schirmer H, Kouyaté B, Müller O (2005) Safety of the combination of chloroquine and methylene blue in healthy adult men with G6PD deficiency from rural Burkina Faso. Trop Med Int Health: TM&IH 10(1):32–38

Meissner PE, Mandi G, Coulibaly B, Witte S, Tapsoba T, Mansmann U, Rengelshausen J, Schiek W, Jahn A, Walter-Sack I, Mikus G, Burhenne J, Riedel K-D, Schirmer RH, Kouyaté B, Müller O (2006) Methylene blue for malaria in Africa: results from a dose-finding study in combination with chloroquine. Malar J 5:84

Mohan N, Balasubramanian N, Basha C (2007) Electrochemical oxidation of textile wastewater and its reuse. J Hazard Mater 147(1–2):644–651. https://doi.org/10.1016/j.jhazmat.2007.01.063

Omar FS, Ming HN, Hafiz SM, Ngee LH (2014) Microwave synthesis of zinc oxide/reduced graphene oxide hybrid for adsorption-photocatalysis application. Int J Photoenergy 2014:1–8. https://doi.org/10.1155/2014/176835

Oyewo OA et al (2020) Sawdust-based cellulose nanocrystals incorporated with zno nanoparticles as efficient adsorption media in the removal of methylene blue dye. ACS Omega 5(30):18798–18807

Pirkanniemi K, Sillanpää M (2002) Heterogeneous water phase catalysis as an environmental application: a review. Chemosphere 48(10):1047–1060. https://doi.org/10.1016/s0045-6535(02)00168-6

Rahimi S, Ehrampoush MH, Ghaneian MT, Reshadat S, Fatehizadeh A, Ahmadian M, Ghanizadeh G, Rahimi S (2013) Application of TiO2/UV-C photocatalytic process in removal of reactive red 198 dye from synthetic textile wastewater. Asian J Chem 25(13):7427–7432. https://doi.org/10.14233/ajchem.2013.14764

Rosi NL, Mirkin CA (2005) Nanostructures in biodiagnostics. Chem Rev 105(4):1547–1562

Roufegari-Nejhad E, Sirousazar M, Abbasi-Chiyaneh V, Kheiri F (2019) Removal of methylene blue from aqueous solutions using poly(vinyl alcohol)/montmorillonite nanocomposite hydrogels: Taguchi optimization. J Polym Environ 27(10):2239–2249. https://doi.org/10.1007/s10924-019-01514-y

Salam HA, Sivaraj R, Venckatesh R (2014) Green synthesis and characterization of zinc oxide nanoparticles from *Ocimum basilicum* L. var. purpurascens Benth.-Lamiaceae leaf extract. Mater Lett 131:16–18. https://doi.org/10.1016/j.matlet.2014.05.033

Schirmer RH, Heiner Schirmer R, Coulibaly B, Stich A, Scheiwein M, Merkle H, Eubel J, Becker K, Becher H, Müller O, Zich T, Schiek W, Kouyaté B (2003) Methylene blue as an antimalarial agent. Redox Rep 8(5):272–275. https://doi.org/10.1179/135100003225002899

Singh P, Kim Y-J, Zhang D, Yang D-C (2016) Biological synthesis of nanoparticles from plants and microorganisms. Trends Biotechnol 34(7):588–599. https://doi.org/10.1016/j.tibtech.2016.02.006

Soren S, Kumar S, Mishra S, Jena PK, Verma SK, Parhi P (2018) Evaluation of antibacterial and antioxidant potential of the zinc oxide nanoparticles synthesized by aqueous and polyol method. Microb Pathog 119:145–151

Talam S, Karumuri SR, Gunnam N (2012) Synthesis, characterization, and spectroscopic properties of ZnO nanoparticles. ISRN Nanotechnol 2012:1–6. https://doi.org/10.5402/2012/372505

Tao Z, Yu X, Liu J, Yang L, Yang S (2008) A facile synthesis and photoluminescence of porous S-doped ZnO architectures. J Alloys Compd 459(1–2):395–398

Velmurugan P, Kumar RV, Dhinakaran G (2011) Dye removal from aqueous solution using low cost adsorbent. Int J Environ Sci 1(7):1492

Vignesh K, Suganthi A, Rajarajan M, Sara SA (2012) Photocatalytic activity of AgI sensitized ZnO nanoparticles under visible light irradiation. Powder Technol 224:331–337

Water & Wastewater (2005) Water for Life: International decade of action begins. Pump Indu Anal 2005(3):3–4. https://doi.org/10.1016/s1359-6128(05)00720-2

World Health Organization. Regional Office for Europe & International Federation of Red Cross and Red Crescent Societies (2001) Infections and infectious diseases: a manual for nurses and midwives in the WHO European region. WHO Regional Office for Europe, Copenhagen. http://apps.who.int/iris/handle/10665/107489

Yuvakkumar R, Suresh J, Joseph Nathanael A, Sundrarajan M, Hong SI (2014) Novel green synthetic strategy to prepare ZnO nanocrystals using rambutan (*Nephelium lappaceum* L.) peel extract and its antibacterial applications. Mater Sci Eng C 41:17–27. https://doi.org/10.1016/j.msec.2014.04.025

Zhang F et al (2013) Adsorption behavior and mechanism of methyl blue on zinc oxide nanoparticles. J Nanopart Res 15(11):2034

Zhao Y, Choi J-W, Bediako JK, Song M-H, Lin S, Cho C-W, Yun Y-S (2018) Adsorptive interaction of cationic pharmaceuticals on activated charcoal: experimental determination and QSAR modelling. J Hazard Mater 360:529–535. https://doi.org/10.1016/j.jhazmat.2018.08.039

Zoungrana A, Coulibaly B, Sié A, Walter-Sack I, Mockenhaupt FP, Kouyaté B, Schirmer RH, Klose C, Mansmann U, Meissner P, Müller O (2008) Safety and efficacy of methylene blue combined with artesunate or amodiaquine for uncomplicated falciparum malaria: a randomized controlled trial from Burkina Faso. PLoS ONE 3(2):e1630